TOXICOLOGICAL SCIENCES **111(2)**, 321–330 (2009)
doi:10.1093/toxsci/kfp174
Advance Access publication July 28, 2009

MRI Characterization of Structural Mouse Brain Changes in Response to Chronic Exposure to the Glufosinate Ammonium Herbicide

Sandra Meme,*[,1,2] André-Guilhem Calas,†[,2] Céline Montécot,† Oliver Richard,† Hélène Gautier,†[,3] Thierry Gefflaut,‡ Bich Thuy Doan,* William Même,* Jacques Pichon,† and Jean-Claude Beloeil*

*Centre de Biophysique Moléculaire, CNRS UPR4301, Orléans, France; †Laboratoire de Neurobiologie, Université d'Orléans, Orléans, France; and ‡Synthèse et étude de systèmes à intérêt biologique UMR 6504, Clermont Ferrand, France

Received April 30, 2009; accepted July 6, 2009

Glufosinate ammonium (GLA) is the active component of herbicides widely used in agriculture, truck farming, or public domains. GLA acts by inhibiting the plant glutamine synthetase (GlnS). It also inhibits mammalian GlnS *in vitro* and *ex vivo*. In the central nervous system this enzyme is exclusively localized in glial cells. Whereas acute neurotoxic effects of GLA are well documented, long-term effects during chronic exposure at low doses remain largely undisclosed. In the present work, C57BL/6J mice were treated intraperitoneally with 2.5, 5, and 10 mg/kg of GLA three times a week during 10 weeks. Cerebral magnetic resonance imaging (MRI) experiments were performed at high field (9.4 T) and the images were analyzed with four texture analysis (TA) methods. TA highlighted structural changes in seven brain structures after chronic GLA treatments. Changes are dose dependent and can be seen at a dose as low as 2.5 mg/kg for two areas, namely hippocampus and somatosensorial cortex. Glial fibrillary acidic protein (GFAP) expression in the same seven brain structures and GlnS activity in the hippocampus and cortex areas were also studied. The number of GFAP-positive cells is modified in six out of the seven areas examined. GlnS activity was significantly increased in the hippocampus but not in the cortex. These results indicate some kind of suffering at the cerebral level after chronic GLA treatment. Changes in TA were compared with the modification of the number of GFAP-positive astrocytes in the studied brain areas after GLA treatment. We show that the noninvasive MRI-TA is a sensitive method and we suggest that it would be a very helpful tool that can efficiently contribute to the detection of cerebral alterations *in vivo* during chronic exposure to xenobiotics.

Key Words: **magnetic resonance imaging; texture analysis; glufosinate ammonium; central nervous system; pesticide; astrocytes.**

Glufosinate ammonium (GLA) is the ammonium salt of the amino acid phosphinotricin (D,L-homoalanin-4-[methyl] phosphinate). GLA is the active component of a broad-spectrum herbicide commercially known as BASTA or LIBERTY (Bayer-Crop Science, Monheim am Rhein, Germany). It is used to control a wide range of weeds in agriculture, public domains, and domestic areas. Introduction of genetically engineered crops, such as corn, cotton, soybeans, canola, rice, sugar beets, resistant to a GLA-containing herbicide has been approved in several countries. In addition, plants naturally resistant to glyphosate (Roundup from Monsanto), another widely used herbicide, begin to emerge in many places around the world (Behrens *et al.*, 2007; Service, 2007). A diversification of herbicides seems to be necessary to raise the selection pressure and give it diversity. For this reason, GLA-containing herbicides could be a valuable alternative. Therefore, it seems reasonable to anticipate a significant increase in the use of GLA-containing herbicides in the next years.

It has been shown that GLA is neurotoxic in acute conditions. This was demonstrated by suicide attempts carried out by ingestion of important quantity of GLA-containing herbicide. These patients developed neurological symptoms such as seizures, convulsions, and loss of memory (Park *et al.*, 2006; Tanaka and Yamashita, 1998; Watanabe and Sano, 1998). In animal models, it has been shown that GLA induces seizures in mice after one intraperitoneal (ip) injection at the dose of 75 mg/kg (Lapouble *et al.*, 2002).

Although acute effects of GLA exposure are well documented (Nakaki *et al.*, 2000; Watanabe and Sano, 1998), results of long-term exposure at low doses remain largely unknown. It has been shown that pesticides of the organophosphate family that includes GLA induce cognitive and neurobehavioral impairments in farm workers (Farahat *et al.*, 2003; Fiedler *et al.*, 1997; Roldan-Tapia *et al.*, 2005). Determination of possible harmful side effects of GLA is a major health concern for people permanently or quasi permanently exposed to the compound. However, only few specific studies have been conducted to appraise the effects of GLA on the central nervous system (CNS) of animals submitted to chronic, low-dose exposure.

In plants, GLA inhibits the activity of the enzyme GlnS leading to a decrease of glutamine and an increase of ammonia

[1] To whom correspondence should be addressed at Centre de Biophysique Moléculaire (CBM CNRS UPR4301), Rue Charles Sadron, 45071 Orléans cedex, France. Fax: +33-2-38-63-15-17. E-mail: sandra.meme@cnrs-orleans.fr.
[2] These two authors contributed equally to this work.
[3] Present address: Department of Veterinary Medicine, University of Cambridge, Cambridge, UK.

which entail the death of the plant (Lea *et al*., 1984). In the CNS of the vertebrates, GlnS (EC 6.3.1.2) plays a key role in the metabolic regulation of glutamate, the major excitatory brain neurotransmitter (Bak *et al*., 2006). Owing that GlnS is exclusively localized in glial cells among which astrocytes represent the major population (Kimelberg and Norenberg, 1989), this makes these astrocytic cells the privileged targets for GLA. Astrocytes can react to many CNS challenges, and reactive astrocytes are the primary hallmarks of many neuropathologies (De Keyser *et al*., 2008). Reactive astrocytes are characterized by a high-level expression of glial fibrillary acidic protein (GFAP) (Wilhelmsson *et al*., 2006).

Magnetic resonance imaging (MRI) is a noninvasive imaging technique which can be used for diagnostic or longitudinal therapeutic purposes. Proton MRI is adapted to study soft material such as cerebral tissue in animal models of human neuropathologies. For instance, MRI has allowed significant progresses in the comprehension of neurological pathologies such as Alzheimer's disease (Braakman *et al*., 2006; Jack *et al*., 2007), epilepsy (Duncan, 2002; Fabene *et al*., 2003; Gröhn and Pitkänen, 2007), multiple sclerosis (Nessler *et al*., 2007; Roosendaal *et al*., 2008), and intracranial tumors (Anderson *et al*., 2005; Fan et al., 2005; Vonarbourg *et al*., 2005). However, MRI studies on small rodents are challenging due to the small sizes of their brains. The recent use of high fields for MRI instruments enables the increase of the spatial resolution, the improvement of the sensitivity of the technique and to optimize the signal-to-noise ratio.

In addition, the heterogeneity of the tissue is one crucial texture parameter that cannot be evaluated with classical optical microscopic methods because of the small size of samples. MRI of an organ *in vivo* and texture analysis (TA) is a way to address that problem. This method gathers several mathematical image analysis methods that enable characterization of an image region of interest (ROI) by studying its constitutive pixels in terms of intensity and spatial distribution. Several different TA methods exist (Haralick, 1979; Lerski *et al*., 1993). They are divided into two different classes: statistical and structural methods (Herlidou *et al*., 1999). In this study we have chosen the statistical ones (histogram, co-occurrence, gradient, and run length matrices). They are well fitted to study tissue without apparent structural regularity. Therefore, a great number of quantitative parameters (more than one hundred) can be extracted from the experiments. Multiparametrical statistical methods such as Correspondence Factorial Analysis (CFA) or Hierarchical Ascending Classification (HAC) are used to pool out texture parameters that aimed identification between different tissue classes. These methods can be used to distinguish healthy from pathological tissues, to follow up the evolution of a pathology or to study the efficacy of therapeutic treatments. Thereby, TA has been successfully applied to cerebral (Herlidou *et al*., 2003; Mahmoud-Ghoneim *et al*., 2003; Yu *et al*., 2002), bone (Herlidou *et al*., 2004; Lespessailles *et al*., 2006; Link *et al*., 1998), muscular (Herlidou *et al*., 1999), and liver (Jirák *et al*., 2002; Zhang *et al*., 2005) tissue in human or animals.

In a previous work (Calas *et al*., 2008) we have shown that chronic exposure to GLA induces structural changes and an increase of GlnS activity in the hippocampus. In this study we have extended our analysis to several other structures in the brain which correspond to visual, auditive, motor, somatosensorial cortex, thalamus, and striatum.

The specific aims of the present study were (1) to appraise the effect of GLA treatment on the structure of the mouse brain by using MRI-TA, (2) to evaluate GFAP expression, whose upregulation is considered as a marker of astrogliosis and neurotoxicity, (3) to compare the structural results obtained with MRI-TA to the results of the cellular and tissue studies obtained by the more classical immunohistochemistry methods.

MATERIAL AND METHODS

Animals and GLA Treatment

Male C57BL/6J mice (25–35 g) obtained from the Centre de Distribution, Typage et Archivage Animal (CDTA, UPS-44, CNRS, Orléans, France) were used. The animals were housed under a 12-h light/dark cycle at constant temperature of 23 ± 1°C with free access to food and water. They were 10 weeks old at the beginning of the treatment. They were divided in four experimental groups of at least five animals each. GLA-treated groups were injected intraperitoneally three times a week with a single dose of GLA solution (2.5, 5, or 10 mg/kg) during 10 weeks according to the previously described protocol (Calas *et al*., 2008). GLA was dissolved in 0.9% saline. The dose was 50 µl/g of mouse. Control animals received a comparable ip injection of 0.9% saline.

The present experimental protocol received full review and approval by the regional animal care and use committee (file number: UNI 45-001/15.10.2005) prior to conducting the experiments. All possible efforts were made to reduce the number of animals studied and to avoid their suffering.

Magnetic Resonance Imaging

All mice underwent MR experiments. They were performed on 9.4 T horizontal magnet dedicated to small animal (94/21 USR Bruker Biospec, Wissembourg, France), equipped with a 950 mT/m gradient set. The mouse head was placed in a linear homogeneous coil (inner diameter: 35 mm). The body temperature (36°C) was maintained constant during the experiments with the help of a warm water circulation heating bed.

The animals were put under gaseous anesthesia during MRI exams (50% N_2O: 0.7 l/min—50% O_2: 0.7 l/min—Isoflurane 1.5%). Breathing rate was monitored during the acquisitions using air pillow placed on the mouse chest to adjust the anesthetic output.

A first series of sagittal images was performed with an eight echoes-Rapid Acquisition with Repeated Echoes sequence (field of view = 1.5 × 1.5 cm, matrix size = 256 × 256, slice thickness = 1 mm, time echo = 46 ms, time repetition = 5 s) leading to an in plane spatial resolution of 59 × 59 µm. Then, 15 axial images were acquired with the same sequence but with a slice thickness of 0.5 mm. The typical MR acquisition duration was 50 min. The central slice of the 15 axial images package always corresponded to the Bregma −0.94 mm so that the position of the slices was reproducible for all mice.

MR Images TA

Acquired MR images were transferred onto an external computer for data processing. The images were normalized. Seven ROIs were selected in both hemispheres and drawn manually on each axial slice to be analyzed. They

TABLE 1
Summary of the TA Methods Used and the Parameters they Provide

TA methods	Available texture parameters
Gray levels histogram	Mean
	Standard deviation
	Skewness
	Kurtosis
	Percentiles 1%, 10%, 50%, 90%, 99%
Co-occurrence matrix ($d = 1$, $\theta = 0°, 45°, 90°, 135°$)	Contrast
	Correlation
	Entropy
	Homogeneity
	Energy
Run length matrix ($\theta = 0°, 45°, 90°, 135°$)	Gray level distribution
	Run distribution
	Long run emphasis
	Short run emphasis
	Run fraction
Gradients matrix	Mean
	Standard deviation

Note. d = distance between the pixels centers in the pattern (i.e., 59 μm in our study), θ = orientation of the pattern.

corresponded to visual, auditive, motor, somatosensorial cortex, hippocampus, thalamus, and striatum. ROI was then analyzed with a home-made software which includes several image TA methods: gray level histogram (order 1), co-occurrence and gradient matrices (order 2), and run length matrix (superior order). These four methods consisted of selecting patterns on the images. They are formed by one or several pixels and in a particular direction.

The order of the method corresponds to the length of the pattern. In our study, patterns formed by two pixels (for the co-occurrence matrix) and in 0°, 45°, 90°, and 135° from the horizontal axis, were chosen. For each orientation, several parameters were calculated. They are summarized in Table 1. Following image analyses, each ROI was characterized with its own texture profile defined with the calculated texture parameters such as contrast, homogeneity, or entropy.

Texture Profiles Analysis

The next step was the establishment of the multiparametric statistical HAC and CFA analyses to compare the different texture profiles following chronic treatment (control, GLA 2.5, 5, and 10 mg/kg) with Xlstat software (Xlstat7.5 ©1995–2004, Addinsoft, Paris, France). Multiparametric analyzes were performed in two steps: first, two-classes HAC (analysis 1) were performed with all of the texture parameters to compare the effect of GLA (control, GLA 2.5, 5, and 10 mg/kg) in pairs on texture profiles. χ^2 tests were then performed to evaluate the robustness of the method in order to compare the number of well-classified ROIs (each ROI corresponds to the texture profile of one mouse) in those two classes. This was repeated for the seven different cerebral structures.

The second step (analysis 2) consisted to establish a possible dose effect and to determine the minimal dose to produce cerebral structural changes detectable with TA methods. For this experiment, several CFA and then four-classes, three-classes, and two-classes HAC were performed to discriminate between profiles generated with the different GLA doses. Analysis 2 was also performed on the seven cerebral ROI. The statistical significance level was set to 0.05 (5%). This second step was also used to choose the most discriminating texture parameters. Indeed, among all the calculated parameters some of them were redundant.

For analysis 2, global value ([true negative + true positive]/total number of ROI) of the test was calculated. It corresponds to the correctly classified ROI in each class. Figure 1 summarizes the different steps all along the TA process.

GlnS Activity Assay

Photometric determination of GlnS activity was based on the formation of an L-γ-glutamylhydroxamate ferric chloride complex and was performed according to Wellner and Meister (1996) with slight modifications. Animals were sacrificed by cervical dislocation. Samples of hippocampus and cerebral cortex were removed from each animal brain kept at 0°C. Tissues were frozen using liquid nitrogen and stored at −20°C until use. Next, the sample was sonicated in a 150mM/5mM KCl/cysteine solution. Homogenates were incubated for 10 min at 37°C, centrifuged 30,000 × g for 1 h, 30 min at 4°C and supernatant was used to dose GlnS activity. The assay mixture consisted of 100mM imidazole at pH 7.2, 50mM sodium L-glutamate, 10mM β-mercaptoethanol, 20mM sodium ATP, 40mM $MgCl_2$, and 100mM hydroxylamine at pH 7.2. The reaction was initiated by the addition of 75 μl of the reactive mixture to 50 μl of the supernatant of each sample. The reaction was quenched after 1 h at 37°C with 150 μl of 0.37M $FeCl_3$/0.67M HCl/0.2M trichloroacetic acid. The reactive mixture was then incubated for 30 min at 4°C before the absorbance was read at 530 nm. All absorbances were within the linear range of the γ-glutamylhydroxamate standard curve. Protein concentration was determined with a dye-binding assay (DC Protein Assay, BioRad, Marne-la-Coquette, France) using bovine serum albumin (BSA) as a standard.

For each animal, concentration determinations were performed in triplicate. GlnS activity was expressed in mM of γ-glutamylhydroxamate formed per hour per mg of proteins at 37°C.

Immunohistochemistry

Animals. Animals were deeply anesthetized with isoflurane and perfused through the heart left ventricle with cold saline solution containing 50 IU/ml of heparin followed by a fixative solution containing 4% paraformaldehyde in 0.1M phosphate buffer (pH 7.4).

Brains were removed and kept in the same cold fixative solution during 16 h at 4°C and cryoprotected with 30% wt/vol sucrose in 0.1M phosphate buffer (pH 7.4) during 24 h at 4°C. Brains were frozen in −50°C isopentane during 1 min.

Coronal 20-μm-thick brain sections were cut on a cryomicrotome (Leica CM3050S, Nanterre, France) −0.7 mm, −1.22 mm, −1.94 mm, −2.92 mm, and −4.16 mm from Bregma. Three contiguous sections were put on a Superfrost Plus slide, air-dried for at least 10 min. Each section was encircled with a hydrophobic pap pen in order to incubate the section in 100 μl of solution (see below).

Anti-GFAP immunohistochemistry. Sections were first rinsed with phosphate-buffered saline (PBS) for 10 min. After incubation in PBS containing 0.4% normal goat serum (NGS), 0.15% Triton X-100, and 1% BSA for 45 min at room temperature, sections were incubated with GFAP polyclonal rabbit antibody (1:500 dilution, Dako-France, Trappes, France) in PBS containing 0.4% NGS and 0.15% Triton X-100 for 12 h at 4°C. For each brain one section was incubated without primary antibody in order to check the specificity of the anti-GFAP labeling. The sections were then rinsed twice with PBS for 10 min and incubated with goat anti-rabbit fluorescein isothiocyanate-labeled antibody (1:100 dilution, Sigma F-9887, Sigma-Aldrich, Saint-Quentin Fallavier, France) for 1 h under cover. Sections were rinsed three times with 0.1% BSA in PBS and finally cover slipped after the deposit of one drop of home-made antifading agent.

GFAP-positive cells counting. Images were acquired digitally on a fluorescence microscope (Nikon Eclipse 80i, Nikon, Champigny sur Marne, France) with DXM 1200F camera (Nikon). Data were taken from four to six animal brains. In brief, video microscope images of histological sections were captured with the Mercator software (Explora Nova, La Rochelle, France). For each five coronal brain sections level a framework was drawn: seven structures were outlined according to Paxinos and Franklin (2001), namely hippocampus, thalamus, striatum, motor cortex, auditive cortex, visual cortex, and somatosensorial cortex.

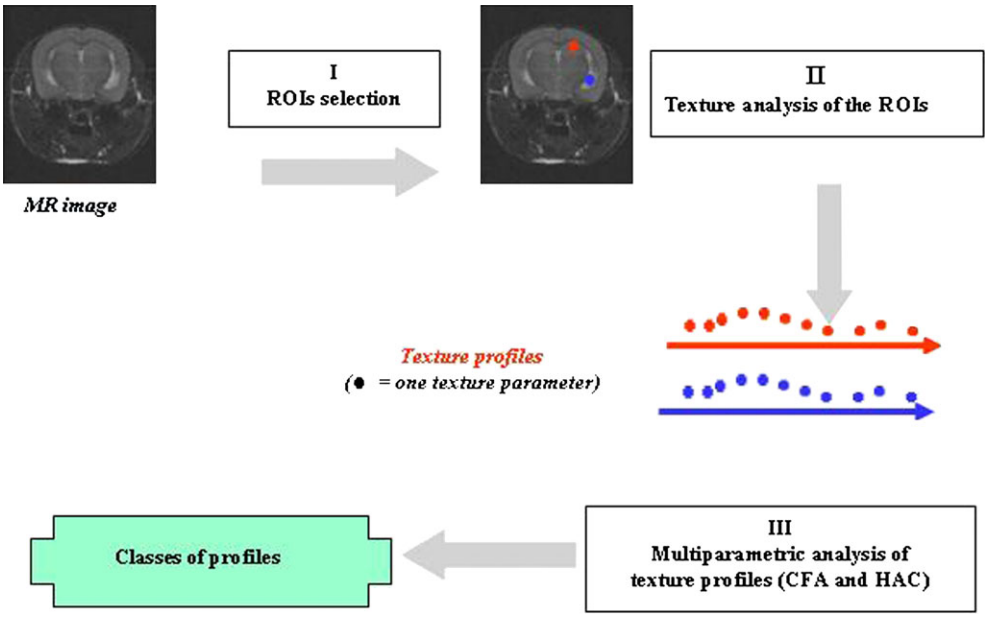

FIG. 1. Scheme of the TA process for an image analysis.

For each level, a fixed number (1–4) of squares (200 × 200 μm) for each structure were drawn with Mercator (Fig. 2). Cells count was carried out with the Image J (rsbweb.nih.gov/ij/ [Bethesda, Maryland]) plug-in Cell counter. Only cells displaying an intense staining with a well-preserved cellular structure and cells straddling top or left square surround were counted. Finally, the mean of GFAP-positive cells of each structure was divided by the sum of the squares surfaces. Each value is expressed as mean (cell number/mm^2) ± SEM.

According to the Kolmogorov-Smirnov test results, our GFAP-positive cells densities did not respond to a standard normal distribution which forced us to evaluate the GFAP staining results by the nonparametric Kruskall-Wallis test followed by the Mann-Whitney test with treatment as between-subject factor.

RESULTS

MRI and TA

Following MRI acquisitions, ROIs corresponding to seven brain structures were selected and their corresponding texture profiles were statistically analyzed by CFA/HAC methods.

Pair comparison between texture profiles (analysis 1) (control vs. 2.5, control vs. 5, control vs. 10, 2.5 vs. 5, 2.5 vs. 10 and 5 vs. 10 mg/kg) is shown in Table 2. The sizes (number of well-classified mice texture profiles) of the two classes (“control” and “GLA 2.5 mg/kg”) are only statistically different in their χ^2 test ($p < 0.05$) for the somatosensorial cortex and the hippocampus. This result suggests that changes in structural organization induced by low doses of GLA are detected at first in these structures. The sizes of the classes are statistically different with higher GLA concentrations (control vs. 5, control vs. 10, 2.5 vs. 5 and 2.5 vs. 10 mg/kg) with better significance level ($p = 0.001$ or $p = 0.0001$) for all cerebral structures.

In addition, the sizes of the classes “GLA 5 mg/kg” versus “GLA 10 mg/kg” are statistically different except for the auditive cortex, the hippocampus, and the striatum ($p > 0.05$) suggesting that maximal effect was probably reached at 5 mg/kg.

Results of the analysis 2 (search for a dose effect) are presented in Figure 3 (CFA), and Figure 4 (HAC). The various CFAs allow eliminating redundant texture parameters. Thereby, only relevant parameters were selected to discriminate ROIs with a statistical p value of 0.05. More than a hundred parameters were available after computing the

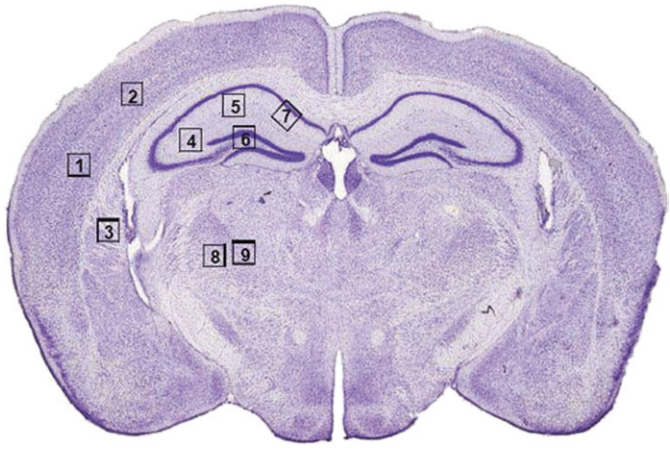

FIG. 2. Drawings of a representative section (Bregma −1.94 mm) used for quantification of GFAP-positive cells. Squares indicate the 200 × 200 μm areas counted inside each structure.

TABLE 2
Results of Two-Classes HAC of Texture Profiles by Comparing Different GLA Doses in Pairs and the Corresponding χ^2 Test *p* Value

	χ^2 test, p value
Control versus GLA 2.5 mg/kg	$p < 0.05$ for somatosensorial cortex and hippocampus
Control versus. GLA 5 mg/kg	$p = 0.0001$ for all structures
Control versus GLA 10 mg/kg	$p = 0.0001$ for all structures
GLA 2.5 mg/kg versus 5 mg/kg	$p = 0.001$ for all structures
GLA 2.5 mg/kg versus 10 mg/kg	$p = 0.0001$ for all structures
GLA 5 mg/kg versus 10 mg/kg	$p < 0.05$ for visual, motor, somatosensorial cortex, thalamus

various TA methods. The choice of the most discriminative parameters is part of the CFA and is made through the determination of the contribution of each parameter to the factorial axes (axes of the CFA in plane representation). Thereby, four of them were kept: contrast, sum average, sum variance (from the co-occurrence matrix), run length distribution (from run length matrix). CFAs were performed for the seven brain structures. After establishing four-classes, three-classes, and then two-classes CFAs, the one that gave the best results (i.e., giving the least unclassified profiles) was obtained with two-clusters CFA. In the hippocampus and the somatosensorial cortex, there are two distinct clusters: one which gathers control texture profiles and another one with GLA 2.5, 5, and 10 mg/kg. In contrast, in the five other brain structures, there is one cluster which gathers control texture profiles and GLA 2.5 mg/kg, and another one which aggregates the texture profiles for GLA 5 mg/kg and 10 mg/kg. For example, the CFA representation for the motor cortex is shown in Figure 3. The graph is given with the two first factorial axes, which include 95.36% of the whole data set (81.20% on factorial axis 1 and 14.17% on factorial axis 2).

Factorial axes 1 and 2 are weighted by contrast 40 and 4%, sum variance 35 and 32%, sum average 13 and 2% and gray level distribution 12 and 62%, respectively. This graph underlines two groups: one is containing ROIs for "control" and "GLA 2.5," the other one containing ROIs for dose 5 and 10 mg/kg. The 2D representation of the two-classes CFA was repeated for all cerebral structures.

Figure 4 is a dendrogram presentation of the HAC analysis of two brain structures corresponding to motor (Fig. 4A) and somatosensorial (Fig. 4B) cortex textures. In Figure 4A one can see that there is a class I (CI) gathering the control (26/26) and 2.5 mg/kg (30/30) texture profiles, whereas class II (CII) gathers texture profiles for 5 (38/38) and 10 mg/kg (26/26). In Figure 4B one can see that there is a class I (CI) gathering the control (32/32), whereas class II (CII) gathers texture profiles for 2.5 mg/kg (36/36), 5 mg/kg (49/49), and 10 mg/kg (34/34).

GlnS Activity in Hippocampal and Cortical Areas

Basal GlnS activities in control mice are 0.23 ± 0.02 and 0.55 ± 0.03mM γ-glutamylhydroxamate formed/h/mg protein for hippocampal and cortical areas, respectively. In the hippocampus, a significant increase in the GlnS activity of 2.73- and 2.46-fold was found after treatment of mice with 5 or 10 mg/kg GLA, respectively. There is no significant increase in the cortical area (Table 3).

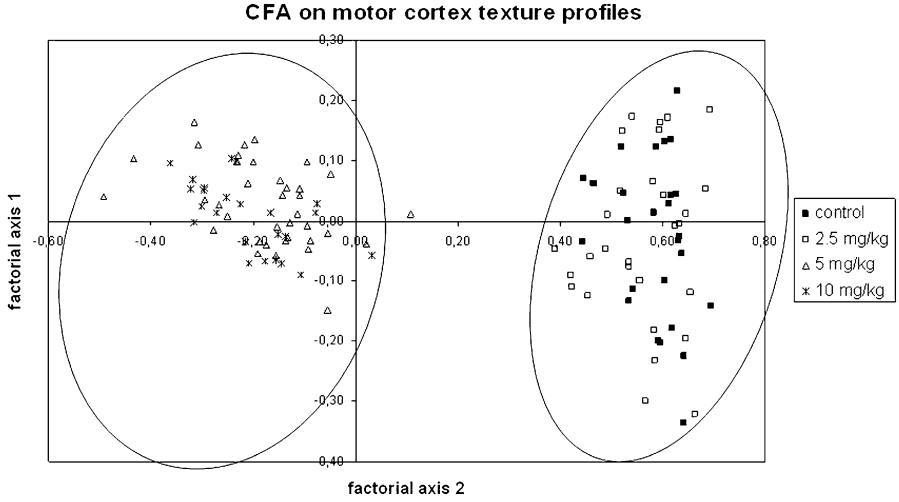

FIG. 3. CFA of the motor cortex ROI for all mice and for control, GLA 2.5, 5, and 10 mg/kg.

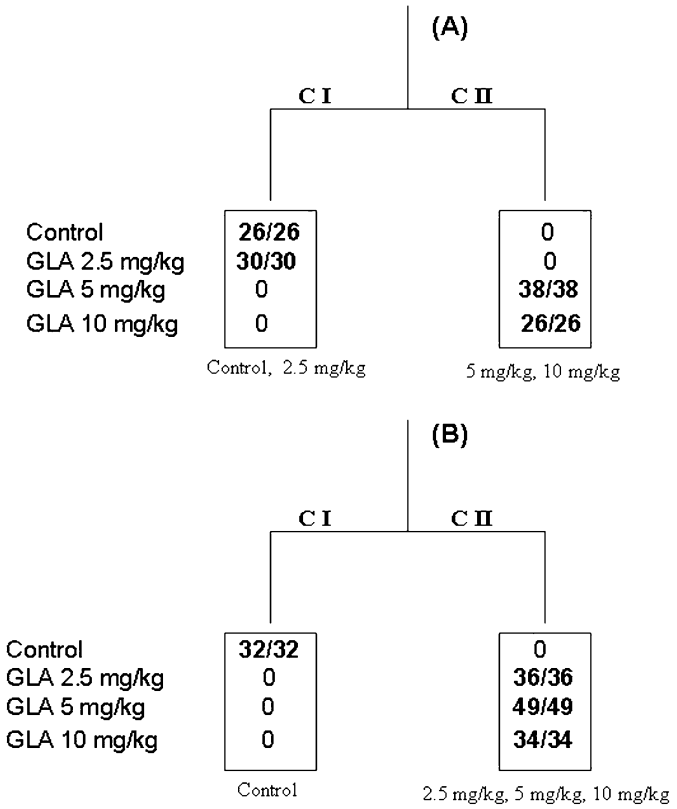

FIG. 4. Representative HAC graph for two brains areas among seven: (A), motor cortex: cluster I (CI) gathers 26/26 and 30/30 texture profiles from control and GLA 2.5 mg/kg treated mice, respectively; cluster II (CII) gathers 38/38 and 26/26 texture profiles from GLA 5 and 10 mg/kg treated mice, respectively. (B), somatosensorial cortex: CI gathers 32/32 texture profiles from control mice and CII texture profiles from GLA 2.5 (36/36), 5 (49/49), and 10 mg/kg (34/34) treated mice.

Number of GFAP-Positive Astrocytes after GLA Treatment

Seven brain regions, namely hippocampus, striatum, visual cortex, motor cortex, somatosensorial cortex, auditive cortex, and thalamus, were examined for their content in GFAP-positive cells. After immunolabeling (see motor cortex staining as an example [Fig. 5]), quantification of GFAP-positive cells was performed as described in the experimental procedure paragraph. Results obtained are shown in Figure 6. Hippocampus is the richest region in GFAP-positive cells with a value of 452 ± 36 cells/mm^2 in control-treated mice, whereas poorest regions are somatosensorial and auditive cortex with less than 50 GFAP-positive cells/mm^2.

In all studied regions, with two exceptions, namely thalamus and auditive cortex, significant modifications of GFAP-positives cell density were observed after GLA treatment. Three regions, specifically somatosensorial, visual, and motor cortex, behave similarly with a dose response-like effect. More particularly, the increase was significant between (1) control-treated mice in visual cortex and 2.5 mg/kg GLA-treated group (+95%); (2) control-treated group and 10 mg/kg GLA-treated group in visual (+300%) and motor cortex (+163%); and (3) 2.5 mg/kg versus 10 mg/kg GLA-treated group in motor cortex (+213%).

Striatum and hippocampus regions display a bell shape pattern with a significant increase between control-treated group and 2.5 or 5 mg/kg GLA-treated group of +25% (hippocampus) and +83% (striatum), respectively.

TABLE 3
GlnS Activity (following 10 Weeks GLA Treatments) Expressed as Percentage of Control

	Cortex	Hippocampus
2.5 mg/kg dose	193% ± 58	167% ± 29
5 mg/kg dose	163% ± 58	273% ± 64*
10 mg/kg dose	147% ± 28	246% ± 58*

Note. The results are expressed as mean percentage ± SEM; *$p \leq 0.05$.

DISCUSSION

The present study demonstrates that chronic exposure at low dose of GLA-induced structural changes paralleled with modification in the number of GFAP-positive astrocytes, in several brain areas of mice. These results obtained with MRI-TA reinforce our previous observations drawn for the chronic effect of GLA on mice hippocampus (Calas *et al*., 2008). To our knowledge, this is the first study which combines a noninvasive imaging MRI-TA method and an immunohistochemistry method, which is the gold standard to evaluate tissue changes or damages during pathologies, pharmacological treatments or as in our case, pesticide exposures. Only very few MRI and magnetic resonance spectroscopy (MRS) studies have been published in the neurotoxicological field to evaluate the impact of pesticides or heavy metal on the CNS. They concerned morphological, not structural, changes of the hippocampus and ventricles size modifications. Park *et al*. (2006) reported a case of human poisoning with an acute dose of GLA. In this study the MR images revealed bilateral lesions in the hippocampus. Moussa *et al*. (2008) showed an enlargement of ventricles and degenerative changes in the striatum of mice treated with the pesticide rotenone, with a 7T MRI device. Jiang *et al*. (2008) with a 3T MR spectrometer revealed a decrease in hippocampus volume for workers exposed to lead.

Our study was performed on mice with a 9.4T device allowing acquisition of high resolution images 59 × 59 μm with a slice thickness of 500 μm. This is a major advantage that permits to highlight very small changes in damaged brain tissues. Working with high field has allowed us to increase image resolution without increasing the acquisition duration which is an important point when working with live animals of small size.

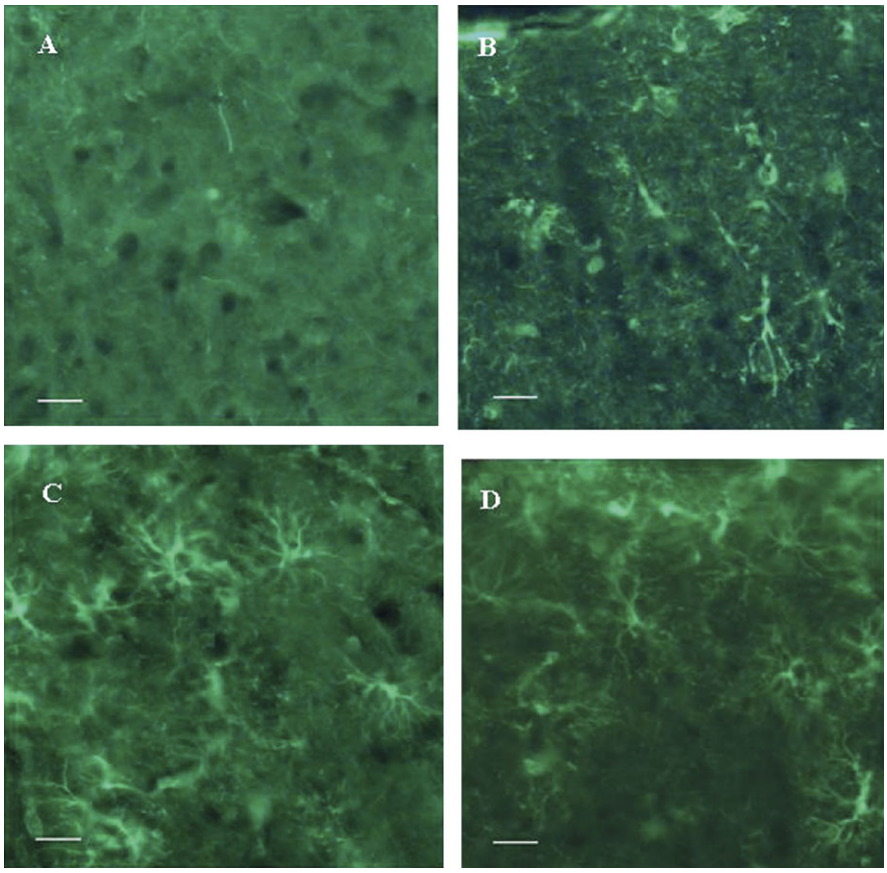

FIG. 5. Histologic sections of GFAP immunoreactivity in motor cortex of mice (A: Control, B: GLA 2.5 mg/kg, C: GLA 5 mg/kg, D: GLA 10 mg/kg. Scale bar = 20 μm).

By using MRI-TA we were able to reveal structural changes in all studied brain structures, whose modifications were not visible on raw MR images. Results also highlighted a dose-dependent effect of GLA treatments with different thresholds of 2.5 mg/kg GLA in the hippocampus and the somatosensorial cortex and 5 mg/kg in the other brain structures, causing significant structural alterations in the brain.

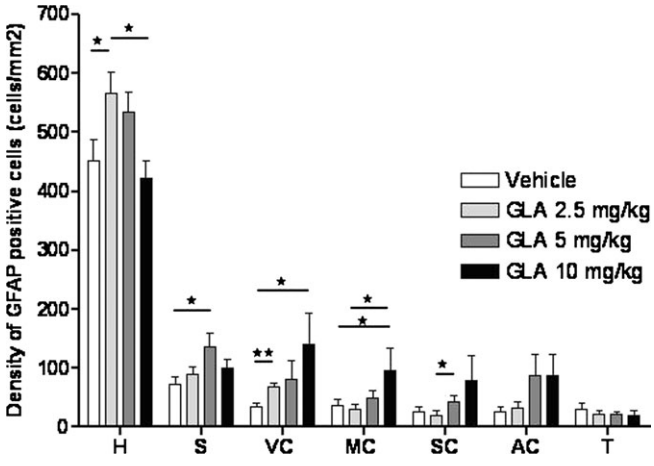

FIG. 6. GFAP-positive cell density of 7 brain areas (H: Hippocampus, S: Striatum, VC: Visual Cortex, MC: Motor Cortex, SC: Somatosensory Cortex, AC: Auditive Cortex, T: Thalamus) after 10 weeks of GLA treatment. Results are expressed as cells/mm^2 ± S.E.M. (n = 9, 8, 9, 9, respectively for the control, GLA 2.5 mg/kg, 5 mg/kg, and 10 mg/kg groups). *$p < 0.05$; **$p < 0.01$.

In order to compare TA results with histological modifications, we have used GFAP labeling as the hallmark of reactive astrocytes. By this means we have shown that, after GLA treatment, five out of the seven cerebral regions studied displayed modifications of the number of GFAP-positive cells. There is a significant increase in the number of reactive astrocytes in the cortical areas, except auditive cortex, with the amount of GLA during treatment. For the striatum and hippocampus, the number of reactive astrocytes peaks at intermediate doses of GLA. It is generally well accepted that an increase in the number of GFAP-positive cells corresponds to a reactive gliosis (Pekny and Nilsson, 2005). So far, astrocyte activation has been described mainly in acute and aggressive pathogenesis, such as stroke, ischemia, trauma, tumor genesis, infections, neurodegenerative diseases (De Keyser *et al.*, 2008; Pekny and Nilsson, 2005), or in physiological aging of the brain (Castillo-Ruiz *et al.*, 2007). Little is known about astrocytes' reactivity after chronic exposure to low level of xenobiotics, such as pesticides. In this study, we have shown

modification in the number of GFAP-positive astrocytes after GLA treatment in several brain areas, revealing some injury at the cerebral level.

In the present study, cellular and structural modifications in different brain areas are revealed by GFAP expression and MRI-TA, respectively. Our results suggest some level of correlation between astrocytes activation and MRI-TA changes in several cerebral structures. But they do not show a strict correlation between TA results and modifications of GFAP expression. Indeed, for example, thalamus seems to behave differently from the other areas studied: no modification in the number of GFAP-positive astrocytes but alteration of MRI-TA patterns after 2.5, 5, and 10 mg/kg GLA treatments. Also we were able to see MRI-TA modifications in the hippocampus at all doses of GLA tested, whereas GFAP expression after 5 and 10 mg/kg GLA treatment, is not significantly different from control mice. MRI-TA changes may be associated with modifications in water environment, intracellular structure organization, and molecular content and distribution (Mahmoud-Ghoneim *et al*., 2003; Roch *et al*., 2002). From our results, it seems reasonable to state that MRI-TA modifications result from stressful conditions and metabolic changes induced by GLA treatment. Indeed GLA may change glutamate metabolism by interfering with GlnS. As previously shown (Calas *et al*., 2008), we have confirmed that chronic treatment of mouse with GLA increases hippocampal GlnS activity. GLA can induce an imbalance between Glu, Gln, and GABA that are metabolically interlink in the brain. A perturbation in the glutamate/glutamine balance could lead to astrocytic swelling (Pekny and Nilsson, 2005). Astrocytes swelling may be achieved by different means (Kimelberg, 2005) among which glutamine seems to play a major role (Albrecht and Norenberg, 2006; Jayakumar *et al*., 2006). In our study, TA changes may be not only due to modification of GFAP expression but also due to changes in intracellular glutamate metabolites contents and astrocytes swelling. A way to study modifications of intracellular molecular content, and more particularly cerebral metabolites specific to neurons and astrocytes after chronic GLA treatment would be to use MRS. This work is presently underway.

In conclusion, our results indicate some kind of suffering at the cerebral level after chronic GLA treatment. Assuming that treatment of mice with 2.5, 5, and 10 mg/kg, three times a week would correspond to a daily intake (DI) of 1.1, 2.1, and 4.3 mg/kg, respectively, the doses of GLA used in the present study are relevant to human environmental exposure and comparable to the Acceptable Daily Intake (ADI) estimated by the World Health Organization (WHO) and the Food and Agricultural Organization (FAO) (J.M.P.R. report, 1999). Indeed, the ADI estimated by WHO and FAO for human is 0.02mg/kg. This value was calculated from the No Observed Adverse Effect Level (NOAEL) for mouse and rat, 11 and 2.1 mg/kg/day, respectively, with a safety factor of 100. We are quite aware that our ip treatment is not absolutely equivalent to food ingestion in term of drug delivery. Nevertheless, considering the NOAEL for mice, here we are using, at the lowest dose (2.5 mg/kg, 3 times a week = 1.1 mg/kg DI), 10 times less GLA. If we make the assumption that the modifications we found in three brain parameters, namely MRI-TA, GlnS activity and GFAP expression, are relevant to brain dysfunction, with our mouse paradigm, NOAEL should be below 1.1 mg/kg/day.

The present study demonstrates that MRI-TA could detect sensitively cerebral alterations following pesticide exposure at low doses. In order to evaluate long-term risk, this noninvasive method is a promising complementary approach to existing tools to detect neurotoxic effects and to follow their evolution during subchronic and chronic toxicological studies.

FUNDING

French National Research Agency (ANR, grant HERBITOX #2006 SEST 18 01); the Centre National de la Recherche Scientifique; and the Université d'Orléans.

ACKNOWLEDGMENTS

The fellowship allocated to A.G.C. by the Région Centre is gratefully acknowledged. We thank J. Moreno and Ph. Moreau for efficient and careful housing of mice. We also thank S. Petoud for careful reading of the manuscript.

REFERENCES

Albrecht, J., and Norenberg, M. D. (2006). Glutamine: A Trojan horse in ammonia neurotoxicity. *Hepatology* **44,** 788–794.

Anderson, S. A., Glod, J., Arbab, A. S., Noel, M., Ashari, P., Fine, H. A., and Frank, J. A. (2005). Noninvasive MR imaging of magnetically labeled stem cells to directly identify neovasculature in a glioma model. *Blood* **105,** 420–425.

Bak, L. K., Schousboe, A., and Waagepetersen, H. S. (2006). The glutamate/GABA-glutamine cycle: Aspects of transport, neurotransmitter homeostasis and ammonia transfer. *J. Neurochem.* **98,** 641–653.

Behrens, M. R., Mutu, N., Chakraborty, S., Dumitru, R., Jiang, W. Z., Lavallee, B. J., Herman, P. L., Clemente, T. E., and Weeks, D. P. (2007). Dicamba resistance: Enlarging and preserving biotechnology-based weed management strategies. *Science* **316,** 1185–1188.

Braakman, N., Matysik, J., Van Duinen, S. G., Verbeek, F., Schliebs, R., de Groot, H. J., and Alia, A. (2006). Longitudinal assessment of Alzheimer's beta-amyloid plaque development in transgenic mice monitored by in vivo magnetic resonance microimaging. *J. Magn. Reson. Imaging* **24,** 530–536.

Calas, A. G., Richard, O., Même, S., Beloeil, J. C., Doan, B. T., Gefflaut, T., Même, W., Crusio, W. E., Pichon, J., and Montécot, C. (2008). Chronic exposure to glufosinate-ammonium induces spatial memory impairments, hippocampal MRI modifications and glutamine synthetase activation in mice. *Neurotoxicology* **29,** 740–747.

Castillo-Ruiz, M. M., Campuzano, O., Acarin, L., Castellano, B., and Gonzalez, B. (2007). Delayed neurodegeneration and early astrogliosis after excitotoxicity to the aged brain. *Exp. Gerontol.* **42,** 343–354.

De Keyser, J., Mostert, J. P., and Koch, K. W. (2008). Dysfunctional astrocytes as key players in the pathogenesis of central nervous system disorders. *J. Neurol. Sci.* **267,** 3–16.

Duncan, J. S. (2002). Neuroimaging for epilepsy: Quality and not just quantity is important. *J. Neurol. Neurosurg. Psychiatry* **73,** 612–613.

Fabene, P. F., Marzola, P., Sbarbati, A., and Bentivoglio, M. (2003). Magnetic resonance imaging of changes elicited by status epilepticus in the rat brain: Diffusion-weighted and T2-weighted images, regional blood volume maps, and direct correlation with tissue and cell damage. *Neuroimage* **18,** 375–389.

Fan, G., Zang, P., Jing, F., Wu, Z., and Guo, Q. (2005). Usefulness of diffusion/perfusion-weighted MRI in rat gliomas: Correlation with histopathology. *Acad Radiol* **12,** 640–651.

Farahat, T. M., Abdelrasoul, G. M., Amr, M. M., Shebl, M. M., Farahat, F. M., and Anger, W. K. (2003). Neurobehavioural effects among workers occupationally exposed to organophosphorous pesticides. *Occup. Environ. Med.* **60,** 279–286.

Fiedler, N., Kipen, H., Kelly-McNeil, K., and Fenske, R. (1997). Long-term use of organophosphates and neuropsychological performance. *Am. J. Ind. Med.* **32,** 487–496.

Gröhn, O., and Pitkänen, A. (2007). Magnetic resonance imaging in animal models of epilepsy-noninvasive detection of structural alterations. *Epilepsia* **48** (Suppl. 4), 3–10.

Haralick, R. M. (1979). Statistical and structural approach to textures. *Proc. IEEE* **67,** 786–804.

Herlidou, S., Constans, J. M., Carsin, B., Olivié, D., Eliat, P. A., Nadal-Desbarats, L., Gondry, C., Le Rumeur, E., Idy-Peretti, I., and de Certaines, J. D. (2003). MRI texture analysis on texture test objects, normal brain and intracranial tumors. *Magn. Reson. Imaging* **21,** 989–993.

Herlidou, S., Grebe, R., Grados, F., Lecuyer, N., Fardellone, F., and Meyer, M. E. (2004). Influence of age and osteoporosis on calcaneus trabecular bone structure. A preliminary in vivo MRI study by quantitative texture analysis. *Magn. Reson. Imaging* **22,** 237–243.

Herlidou, S., Rolland, Y., Bansard, J. Y., Le Rumeur, E., and de Certaines, J. D. (1999). Comparison of automated and visual texture analysis in MRI: characterization of normal and diseased skeletal muscle. *Magn. Reson. Imaging* **17,** 1393–1397.

Jack, C. R., Marjanska, M., Wengenack, T. M., Reyes, D. A., Curran, G. L., Lin, J., Preboske, G. M., Poduslo, J. F., and Garwood, M. (2007). Magnetic resonance imaging of Alzheimer's pathology in the brains of living transgenic mice: A new tool in Alzheimer's disease research. *Neuroscientist* **13,** 38–48.

Jayakumar, A. R., Rao, K. V., Murthy, C. R., and Norenberg, M. D. (2006). Glutamine in the mechanism of ammonia-induced astrocyte swelling. *Neurochem. Int.* **48,** 623–628.

Jiang, Y. M., Long, L. L., Zhu, X. Y., Zheng, H., Fu, X., Ou, S. Y., Wei, D. L., Zhou, H. L., and Zheng, W. (2008). Evidence of altered hippocampal volume and brain metabolites in workers occupationally exposed to lead: A study by magnetic resonance imaging and 1H magnetic resonance spectroscopy. *Toxicol. Lett.* **181,** 118–125.

Jirák, D., Dezortová, M., Taimr, P., and Hájek, M. (2002). Texture analysis of human liver. *J. Magn. Reson. Imaging* **15,** 68–74.

J. M. P. R. report. (1999). Pesticide residues in food. Report of the Joint Meeting of the FAO Panel of Experts on Pesticide Residues in Food and the Environment and the WHO Core Assessment Group. FAO Plant Production and protection. Paper #153, 1999. Available at: http://www.fao.org/ag/AGP/AGPP/Pesticid/JMPR/Download/99_rep/REPORT1999.pdf. Accessed August 11, 2009.

Kimelberg, H. K. (2005). Astrocytic swelling in cerebral ischemia as a possible cause of injury and target for therapy. *Glia* **50,** 389–397.

Kimelberg, H. K., and Norenberg, M. D. (1989). Astrocytes. *Sci. Am.* **260,** 66–72.

Lapouble, E., Montecot, C., Sevestre, A., and Pichon, J. (2002). Phosphinothricin induces epileptic activity via nitric oxide production through NMDA receptor activation in adult mice. *Brain Res.* **957,** 46–52.

Lea, P. J., Joy, K. W., Ramos, J. L., and Guerrero, M. G. (1984). The action of 2-amino-4-(methylphosphinyl)-butanoic acid (phosphinothricin) and its 2-oxo-derivative on the metabolism of cyanobacteria and higher plants. *Phytochemistry* **23,** 1–6.

Lerski, R. A., Straughan, K., Schad, L. R., Boyce, D., Bluml, S., and Zuna, I. (1993). MR image texture analysis—An approach to tissue characterization. *Magn. Reson. Imaging* **1,** 873–887.

Lespessailles, E., Chappard, C., Bonnet, N., and Benhamou, C. L. (2006). Imaging techniques for evaluating bone microarchitecture. *Joint Bone Spine* **73,** 254–261.

Link, T. M., Majumdar, S., Lin, J. C., Newitt, D., Augat, P., Ouyang, X., Mathur, A., and Genant, H. K. (1998). A comparative study of trabecular bone properties in the spine and femurusing high resolution MRI and CT. *J. Bone Miner. Res.* **13,** 122–132.

Mahmoud-Ghoneim, D., Toussaint, G., Constans, J. M., and de Certaines, J. D. (2003). Three dimensional texture analysis in MRI: A preliminary evaluation in gliomas. *Magn. Reson. Imaging* **21,** 983–987.

Moussa, C. E., Rusnak, M., Hailu, A., Sidhu, A., and Fricke, S. T. (2008). Alterations of striatal glutamate transmission in rotenone-treated mice: MRI/MRS in vivo studies. *Exp. Neurol.* **209,** 224–233.

Nakaki, T., Mishima, A., Suzuki, E., Shintani, F., and Fujii, T. (2000). Glufosinate ammonium stimulates nitric oxide production through N-methyl D-aspartate receptors in rat cerebellum. *Neurosci. Lett.* **290,** 209–212.

Nessler, S., Boretius, S., Stadelmann, C., Bittner, A., Merkler, D., Hartung, H. P., Michaelis, T., Brück, W., Frahm, J., Sommer, N., *et al.* (2007). Early MRI changes in a mouse model of multiple sclerosis are predictive of severe inflammatory tissue damage. *Brain* **130,** 2186–2198.

Park, H. Y., Lee, P. H. L., Shin, D. H. S., and Kim, G. W. K. (2006). Anterograde amnesia with hippocampal lesions following glufosinate intoxication. *Neurology* **67,** 914–915.

Paxinos, G., and Franklin, K. B. J. (2001). In *The mouse brain in stereotaxic coordinates*, 2nd ed. Academic Press, San Diego, CA.

Pekny, M., and Nilsson, M. (2005). Astrocyte activation and reactive gliosis. *Glia* **50,** 427–434.

Roch, C., Leroy, C., Nehlig, A., and Namer, I. (2002). Magnetic resonance imaging in the study of the lithium-pilocarpine model of temporal lobe epilepsy in adult rats. *Epilepsia* **43,** 325–335.

Roldan-Tapia, L., Parron, T., and Sánchez-Santed, F. (2005). Neuropsychological effects of long-term exposure to organophosphate pesticides. *Neurotoxicol. Teratol.* **27,** 259–566.

Roosendaal, S. D., Moraal, B., Vrenken, H., Castelijns, J. A., Pouwels, P. J., Barkhof, F., and Geurts, J. J. (2008). In vivo MR imaging of hippocampal lesions in multiple sclerosis. *J. Magn. Reson. Imaging* **27,** 726–731.

Service, R. F. (2007). Glyphosate-the conservationist's friend? *Science* **316,** 1116–1117.

Tanaka, J., and Yamashita, M. (1998). Two cases of glufosinate poisoning with late onset convulsions. *Vet. Hum. Toxicol.* **40,** 219–222.

Vonarbourg, A., Sapin, A., Lemaire, L., Franconi, F., Menei, P., Jallet, P., and Le Jeune, J. J. (2005). Characterization and detection of experimental rat gliomas using magnetic resonance imaging. *MAGMA* **17,** 133–139.

Watanabe, T., and Sano, T. (1998). Neurological effects of glufosinate poisoning with a brief review. *Hum. Exp. Toxicol.* **17,** 35–39.

Wellner, V. P., and Meister, A. (1996). Binding of adenosine triphosphate and adenosine diphosphate by glutamine synthetase. *Biochemistry* **5,** 872–879.

Wilhelmsson, U., Bushong, E. A., Price, D. L., Smarr, B. L., Phung, V., Terada, M., Ellisman, M. H., and Pekny, M. (2006). Redefining the concept of reactive astrocytes as cells that remain within their unique domains upon reaction to injury. *Proc. Natl. Acad. Sci. U. S. A.* **103,** 17513–17518.

Yu, O., Mauss, Y., Zollner, G., Namer, I. J., and Chambron, J. (2002). Distinct patterns of active and non-active plaques using texture analysis on brain NMR images in multiple sclerosis patients: Preliminary results. *Magn. Reson. Imaging* **17,** 1261–1267.

Zhang, X., Fujita, H., Kanematsu, M., Zhou, X., Hara, T., Kato, H., Yokoyama, R., and Hoshi, H. (2005). Improving the classification of cirrhotic liver by using texture features. *Conf. Proc. IEEE Eng. Med. Biol. Soc.* **1,** 867–870.